AAEC/E172

AAEC/E172

AUSTRALIAN ATOMIC ENERGY COMMISSION
RESEARCH ESTABLISHMENT
LUCAS HEIGHTS

PROMPT NUBAR MEASUREMENTS FOR THERMAL NEUTRON FISSION

by

J. W. BOLDEMAN
A.W. DALTON

March 1967

AUSTRALIAN ATOMIC ENERGY COMMISSION

RESEARCH ESTABLISHMENT

LUCAS HEIGHTS

PROMPT NUBAR MEASUREMENTS FOR THERMAL NEUTRON FISSION

by

J. W. BOLDEMAN

A. W. DALTON

ABSTRACT

The number of prompt neutrons ($\bar{\nu}$) produced in the thermal neutron induced fission of U233, U235, Pu239, and Pu241 has been determined with high accuracy using the liquid scintillator technique. Measurements were made relative to an assumed value of $\bar{\nu}$ = 3.784 for the spontaneous fission of Cf252. The present results are compared with previous measurements.

CONTENTS

(continued)

CONTENTS (continued)

1. INTRODUCTION

Accurate measurements of $\bar{\nu}$, the average number of neutrons produced per fission event, for the fissile isotopes are needed to calculate accurately the behaviour of a reactor system. Relative measurements are made by comparing the $\bar{\nu}$ value of a particular fissile material with an assumed value of $\bar{\nu}$ for the spontaneous fission of Cf252. Absolute measurements are concerned with the determination of $\bar{\nu}$ for Cf252.

Four independent and highly accurate measurements have been made of absolute $\bar{\nu}$ for Cf252, two using liquid scintillators (Asplund-Nilsson et al. 1963, Hopkins and Diven 1963), one with the Boron Pile (Colvin and Sowerby 1965), and a fourth from a comparison of Cf252 fission neutrons with a calibrated neutron source in a wax castle (Moat et al. 1961). Initially all four results were in good agreement. However, recently the two latter measurements have been revised (Fieldhouse et al. private communication and Colvin and Sowerby 1965) and a discrepancy of about 2 per cent. now exists between the revised measurements and the unmodified ones (Table 1).

TABLE 1

PROMPT $\bar{\nu}$ VALUES FOR Cf252

Original Result	Revised Result	Experiment
3.799 ± 0.034		Asplund-Nilsson et al. (1963)
3.771 ± 0.031		Hopkins and Diven (1963)
3.77 ± 0.07	3.685 ± 0.040	Moat et al. (1961) and Fieldhouse et al. (1966)
3.751 ± 0.038	3.705 ± 0.015	Colvin and Sowerby (1963, 1965)

The discrepancy is such that it does not affect relative measurements and for some isotopes the agreement obtained between all measurements is excellent. For example, the prompt $\bar{\nu}$ value for the thermal neutron induced fission of U235 relative to Cf252 is now known to about 0.2 per cent. The present experiment has been designed not to investigate the discrepancy which exists in the absolute measurements but to improve the relative values for U233, Pu239, and Pu241 to the same accuracy as that for the U235 value.

A value of $\bar{\nu}$ = 3.784 was assumed for the spontaneous fission of Cf252. This value is the weighted mean of the two liquid scintillator measurements and has been used for convenience, since, with this value, relative measurements uf U235, etc., fall into line with values currently in use.

2. THE EXPERIMENTAL METHOD

In the liquid scintillator technique (Mather et al. 1964, Hopkins and Diven 1963) the neutron detector consists of a large liquid scintillator which is loaded with a high neutron cross section material such as gadolinium or cadmium. A fission counter is placed at the centre of a tube which runs axially through the scintillator tank and allows entry and exit of neutrons. Neutrons produced by fission in this counter enter the scintillator, are moderated there and after a mean lifetime, generally of the order of 10 μs, are captured by the gadolinium or cadmium. The capture gamma rays cause scintillations which may be detected by photomultiplier tubes mounted on the outside of the tank. Thus in about 40 μs following fission the majority of the neutrons are detected. Excellent discrimination against background radiation can be obtained by gating the output of the photomultiplier tubes with a pulse from the fission chamber and counting output photomultiplier pulses only during the gating time.

The neutron detection efficiency of such liquid scintillators may be calibrated either by using an assumed value of $\bar{\nu}$ for the spontaneous fission of Cf252 in relative measurements, as was done in the present experiment, or for absolute $\bar{\nu}$ measurements, by using (n,p) scattering for which $\bar{\nu}$ = 1.

The details of the various elements of the experimental set-up used in these measurements are described below:

3. THE FISSION COUNTER

The fission counter was a high speed ionization chamber with a parallel plate spacing of 3 mm, across which a positive voltage of 450 volts was applied (Figure 1). A similar counter has been described by De Volpi et al. (1964). The counting gas, methane, was purified using the technique described by Cunninghame and Kitt (1964).

The fissile foils were prepared by electroplating the particular isotope onto nickel discs (0.006 inches thick). All fission counters consisted of two chambers, one on each side of the nickel discs. However, only in the case of U235 was the double chamber used and then the nickel disc was plated on both sides. Table 2 gives the weights of the fissile targets and Table 3 gives the isotopic concentrations of the enriched isotopes.

TABLE 2

FISSION COUNTER DETAILS

Isotope	No. of Chambers	Weight of Material (mg)
U233	1	2.1
U235	2	8.1
Pu239	1	0.7
Pu241	1	2.8

TABLE 3

ISOTOPIC ANALYSIS OF FISSILE MATERIALS

Isotope / Foil	U233	U234	U235	U236	U238	Pu239	Pu240	Pu241	Pu242
U233	99.27	0.07	0.04	0.07	0.53				
U235		1.28	92.72	0.254	5.75				
Pu239						99.83	0.17		
Pu241						1.44	5.69	91.78	1.09

A fast current amplifier (Rush 1964) was used in conjunction with the fission counters and the output was fed to a tunnel diode discriminator. Typical output pulses from the fast current amplifier had a rise time of 5 ns and a pulse duration of 20 ns (Figure 2). The discriminator output pulses were square and of 25 ns duration. The fission counter was operated in coincidence with the liquid scintillator tank. A genuine fission event was established by a coincidence between a fission counter pulse and a pulse arising from detection of proton recoil and prompt fission gamma rays in the liquid scintillator. A coincidence resolving time of 21 ns was used. The combination of short pulse duration and small coincidence resolving time gave a high discrimination against amplifier noise originating in the fission counter line and alpha pile-up pulses. An investigation of the

performance of the fission counter with a Pu240 spontaneous fission source indicated that alpha pile-up effects were negligible compared with the effects of amplifier noise.

The fission counter bias curve obtained for Cf252 is shown in Figure 3a. The dashed line in Figure 3a is the bias curve obtained with the coincidence restraint removed, allowing the effect of amplifier noise to be observed. The measurements were continued into the region of excessive amplifier noise and are plotted in Figure 3b. The dashed line as before is the bias curve without the coincidence restraint. The dotted line in Figure 3b is the coincidence rate corrected for random coincidence effects. Similar curves were obtained for the fission counters containing U233, U235, Pu239, and Pu241. In all cases an excellent plateau was obtained indicating the adequate elimination of amplifier noise and alpha pile-up and furthermore, the approximately 100 per cent. fission fragment detection efficiency. For relative $\bar{\nu}$ measurements, the discriminator bias was set above the onset of excessive amplifier noise. Under these conditions corrections of about 0.05 per cent. were necessary to account for random coincidence events. The measurement was rejected if a larger correction was necessary.

With the operation conditions as above, fission detection efficiencies of 98 per cent. in the case of Cf252 and 94.5 per cent. in the case of U235 were obtained. The efficiencies for the other isotopes lay within these limits. The effect of less than 100 per cent. fission fragment detection efficiency on the $\bar{\nu}$ measurements is considered in Section 9.

4. THE LIQUID SCINTILLATOR TANK

The liquid scintillator tank (Figure 4) was 76 cm in diameter and held 240 litres of NE323 which contains a loading of 0.5 per cent. by weight gadolinium. Scintillations resulting from neutron capture within the tank were viewed by twelve 5 in. EMI 9618A photomultiplier tubes. To minimize spurious events produced by noise or after pulsing within any one photomultiplier tube, the photomultiplier tubes were connected in three coincident banks of four photomultipliers each with a coincidence resolving time of 25 ns. The particular arrangement of the tubes has been discussed by Moat et al. (1962) who found a longer and flatter curve of neutron efficiency versus E.H.T. with the 3 x 4 arrangement than with a similar 2 x 6 arrangement. An axial tube 3 in. in diameter through the tank allowed the passage of a neutron beam. The appropriate fission counter was centred in this tube.

5. THE NEUTRON SOURCE

A one inch diameter collimated beam of thermal neutrons from the 10 kW UTR-10 reactor MOATA (Marks 1962) was passed through the central hole of the tank; collimation was achieved with lead, graphite, and borated paraffin (Figure 5). Background from reactor and cosmic radiation, was minimized by enclosing the entire tank in 3 feet of heavy concrete. Environmental background was then 0.1 counts/counting gate of 40 μs. The reactor power was limited to 200 watts owing to increasing background. The maximum usable flux at the centre of the scintillator was therefore 2.5×10^3 n cm^{-2} sec^{-1} and the background was 0.7 counts per gate. For the neutron spectrum emerging from the collimator the ratio of thermal neutron fission to fission induced by neutrons above 1 keV was estimated to be about 10^4 so no correction for the fast neutron component of the beam was necessary.

6. ELECTRONICS

The logic of the electronics is shown in Figure 6. The output from each bank of photomultiplier tubes was fed to a tunnel diode discriminator via 100 Mc/s bandwidth amplifiers and thence to the triple coincidence unit. A genuine fission event was established by a coincidence between a prompt gamma-ray pulse in the liquid scintillator and a pulse from the fission counter.

The genuine fission signal was used to initiate a 40 μs gate during which time events from the scintillator tank were recorded in the temporary store. The gate opened approximately 200 ns after the fission event. A gate-time of 40 μs was chosen since 99 per cent. of the detected neutrons were recorded in this time. It was uneconomical to extend the gate-time beyond 40 μs because of the relative increase in background. At the end of each 40 μs gate-time a 100 μs waiting period was introduced after which a 40 μs counting gate was initiated to record background. Background events were also recorded within the temporary store. The 100 μs waiting time was varied to determine any systematic difference introduced by the choice of a specific time. No difference was ever observed.

At the end of the entire counting cycle of 180 μs the contents of the temporary store were transferred to the multiple event counter, provided a second detectable fission event had not occurred during the counting cycle. The detection of a second fission event caused all information in the temporary store to be erased. The elimination of double fission was virtually complete and the error introduced is considered in Section 9. The multiple event counter had 17 channels in all, eleven of which corresponded to occasions on which 0 to 10 events were recorded during the first counting gate, while the remaining six corresponded to 0 to 5 background events during the second gate. The number of channels used was more than adequate to store accurately all multiple events during either counting gate.

7. CALIBRATION OF THE LIQUID SCINTILLATOR TANK

7.1 Gain of Photomultiplier Tubes

The gain of each of the twelve photomultiplier tubes was adjusted to the same value by measuring the ratio of the number of gates to the number of fissions for each tube in coincidence with all the photomultiplier tubes of the remaining two banks. The delay through each photomultiplier tube was adjusted to be the same at the input to the first coincidence unit.

The efficiency of the liquid scintillator tank for fission neutron detection was measured, as a function of voltage to the photomultiplier tubes, by comparing the neutron counts per gate for the spontaneous fission of Cf252 with an assumed value of $\bar{\nu} = 3.784$. The measured curve is shown in Figure 8. The efficiency of the tank reached a value of 85.6 per cent. at 1900 volts. Measurements were not taken beyond this voltage as cosmic ray background tended to overload the amplifiers. The efficiency figures quoted in Figure 8 have not been corrected for overlap of neutron pulses, etc. These corrections are about 1 per cent. During the course of the measurements, the photomultiplier tube discriminators were modified slightly and an efficiency of 89 per cent. was achieved at 1600 volts to the photomultiplier tubes. Despite the availability of this high efficiency, all $\bar{\nu}$ measurements were made at an efficiency of approximately 83 per cent. to minimize the contribution of delayed fission gamma rays (see Section 9.12).

7.2 Variation of Efficiency with Fission Counter Position

The variation in efficiency of the liquid scintillator tank was measured as a function of fission counter position within the centre axial tube (Figure 9). The fission counter could be relocated to within 0.25 cm and any variation in efficiency resulting from location errors was less than 0.01 per cent.

7.3 Variation of Efficiency with Neutron Energy

Values for the variation of neutron detection efficiency with neutron energy have been supplied by A. Moat, D. Mather, and P. Fieldhouse (private communication) from their comparison of the performance of the present scintillator with that of the scintillator at Aldermaston for which the efficiency variation was determined using a Monte Carlo calculation. The two scintillators are exactly the same in size and have essentially the same composition; the present scintillator contains approximately 10 per cent. more hydrogen per cm^3. The neutron efficiency variation obtained from this comparison for several neutron energies is shown in Table 4.

TABLE 4

RELATIVE DETECTOR EFFICIENCY VERSUS NEUTRON ENERGY

Neutron Energy (MeV)	Efficiency
0.3	95.5
0.5	94.9
1.5	94.8
3.0	93.1
5.0	83.4
7.0	77.1
10.0	71.1
14.0	61.1

7.4 Effect of Fission Counter Bias Level

The variation with fission chamber bias of the apparent Cf252 $\bar{\nu}$ value was measured between discriminator bias levels equivalent to 98 per cent. and 5 per cent. fission fragment detection efficiencies. Apparent $\bar{\nu}$ for Cf252 was found to be virtually constant over the entire range. However, there appeared to be a slight increase of approximately 0.2 per cent. at 50 per cent. fission fragment detection efficiency which disappeared below 40 per cent. fission fragment efficiency. At 5 per cent. detection efficiency, apparent $\bar{\nu}$ for Cf252 agreed, within the statistical accuracy of 0.5 per cent., with the 98 per cent. efficiency figures. Interpretation of this small variation would include consideration of the small anisotropy of neutron detection of the scintillator and the effects of the correlation of ν with mass division in fission; this has not been attempted.

The variation does not affect the relative $\bar{\nu}$ measurements as all were made with fission fragment detection efficiencies in excess of 90 per cent.

7.5 Dead Time Correction

The dead time of the neutron counting system was set by the performance of the photo-multiplier tubes. All other counting elements had smaller dead times.

Two different measurements were made of the dead time. In one method the output pulse from the second coincidence unit was divided, a delayed signal fed the start input of a time to pulse height converter and the prompt pulse was fed to the stop input. Figure 7 shows the distribution in time (including the introduced delay time of 24 ns) of a second pulse following the start pulse. The scintillator pulses for this measurement originated from the detection of Pu-Be source neutrons. The Pu-Be source strength was sufficient to swamp the background radiation detection rate. The measured dead time for neutron detection was 73 ns. The dead time was remeasured with the Pu-Be source removed and in the presence of a typical background radiation spectrum as encountered during the $\bar{\nu}$ measurements. A similar curve to that of Figure 7 was obtained except that there was an approximately 3 ns shift towards a smaller dead time. As expected, the dead time was slightly pulse height dependent. The variation was sufficiently small to be ignored for all dead time corrections. The error so introduced was covered many times by the assessed error for the dead time corrections (Section 9.10).

In the second method the number of neutrons detected per spontaneous fission of Cf252 in the presence and absence of a Pu-Be neutron source were compared. Analysis of several measurements indicated that the dead time was 76 $\pm$ 9 ns.

The probability of neutron detection within the liquid scintillator as a function of time after fission was measured by using the fission pulse to trigger a time-to-pulse height converter and using a randomly selected neutron pulse as the stop pulse (Figure 10). The background detection probability with time is constant. These curves were used in conjunction with the measured dead time of 73 ns to correct for pulse overlap. Because the dead time of the counting equipment was very small, it was necessary to consider the correction for double pulse overlap only, and not for higher orders which are at least 50 times less probable. The pulses produced during the neutron counting gate were subject to pulse overlap of three types:

(a) Neutron-neutron overlap.

(b) Neutron-background overlap.

(c) Background-background overlap.

The pulses produced during the background counting gate were subject only to background-background overlap.

If k_{nn} is defined as the probability that two neutron pulses, occurring during the 40 μs gate, overlap and appear as one pulse, then:

$$k_{nn} = 2\tau \int_0^T f^2(t)dt = 0.00675.$$

Here f(t) is the normalized time distribution of capture pulses, (Figure 10), τ is the dead time, and T is the gate time of 40 μs. The probability of overlap of one neutron pulse and one background pulse occurring during the counting gate is defined as k_{nB} where:

$$k_{nB} = 2\tau/T \int_0^T f(t)dt = 2\tau/T = 0.00365 \quad .$$

The probability k_{BB} of overlap of two background pulses is given simply by $2\tau/T$ and is equal to 0.00365 .

If F_ℓ is defined as the probability of occurrence of ℓ events during the neutron counting gate and if D_x and B_x are the probabilities of occurrence of x neutrons and x background events respectively, then:

$$F_\ell = \sum_{x=0}^{\ell} D_x \, B_{\ell-x} \quad .$$

The measured probability of observing ℓ events during the neutron counting gate F'_ℓ will differ from F_ℓ for two reasons.

(a) The probability of overlap of two of the ℓ events is finite and these situations will contribute to the measured $F'_{\ell-1}$ probability.

(b) There will be a contribution to the measured F'_ℓ probability because of overlap in situations where $\ell + 1$ events occurred during the counting gate.

We may therefore write for the measured F'_ℓ probabilities:

$$F'_\ell = \sum_{x=0}^{\ell} D_x \, B_{\ell-x} \, [1 - {}^{x}C_2 \, k_{nn} - x(\ell - x) k_{nB} - {}^{\ell-x}C_2 \, k_{BB}]$$

$$+ \sum_{x=0}^{\ell+1} D_x \, B_{\ell+1-x} \, [{}^{x}C_2 \, k_{nn} + x(\ell + 1 - x) \, k_{nB} + {}^{\ell+1-x}C_2 \, k_{BB}] \quad . \qquad (1)$$

Similarly, for the measured background probabilities B'_x,

$$B'_x = B_x(1 - {}^{x}C_2 \, k_{BB}) + B_{x+1} \, {}^{x+1}C_2 \, k_{BB} \quad . \qquad (2)$$

For each measurement, the sets of equations (1) and (2) were solved on an IBM 7040 computer and the probabilities D_x of observing x neutrons per fission gate corrected for all forms of overlap and with the background removed, were so obtained.

8. RESULTS

Measurements were made of the number of prompt neutrons emitted in the thermal neutron induced fission of U233, U235, Pu239, and Pu241. An assumed value of 3.784 was used for the prompt value of $\bar{\nu}$ for the spontaneous fission of Cf252. The corrected D_x values were combined in the obvious way to obtain first the scintillation tank detection efficiency from the Cf252 results and then the $\bar{\nu}$ values of the above isotopes using this efficiency figure. In other words, for U235, for example,

$$\bar{\nu}\,(U235) = \frac{3.784 \; \Sigma_x \, D_x(U235)}{\Sigma_x \, D_x(Cf252)} \quad .$$

A number of measurements were made for each isotope and the efficiency of the liquid scintillator was calibrated before and after each measurement, using Cf252. The individual results for each of the four sets were statistically consistent. The four results corrected for the various effects discussed in Section 9 together with their accuracy are tabulated in Table 5. In assessing the accuracy no account has been taken of any error in the assumed value of $\bar{\nu}$ for Cf252.

TABLE 5

FINAL PROMPT $\bar{\nu}$ RESULTS RELATIVE TO $\bar{\nu}$ = 3.784 FOR Cf252

Isotope	ν
U233	2.492 ± 0.008
U235	2.416 ± 0.008
Pu239	2.904 ± 0.008
Pu241	2.947 ± 0.007

9. ACCURACY AND CORRECTIONS

Certain corrections must be applied to the measured data and their accuracy contributes to that of the results. Several random effects further limit the accuracy of the measurements. Such considerations are discussed separately below.

Table 6 lists the magnitude of the various corrections and all sources contributing to error in each of the four measurements.

9.1 Statistical Accuracy

The statistical accuracy of the mean number of events per gate, whether they be neutrons or backgrounds, for a particular measurement is given by:

$$\left[\sum_{i=0}^{i_{max}} i^2 g_i - \left(\sum_{i=0}^{i_{max}} i\, g_i \right)^2 \left(\sum_{i=0}^{i_{max}} g_i \right)^{-1} \right]^{\frac{1}{2}} \left[\sum_{i=0}^{i_{max}} g_i \right]^{-1} ,$$

where g_i is the number of gates for which i events were detected. (Mather et al. 1964). The accuracy of a particular measurement of $\bar{\nu}$ was obtained by combining the statistical accuracy of the Cf252 calibration with the statistical accuracies of the mean number of events per gate and the mean number of background events per gate.

A large number of measurements of $\bar{\nu}$ were made for each isotope. The distribution of the $\bar{\nu}$ values within any particular set was consistent with the statistical accuracy of the individual measurements assessed as above. The statistical accuracies of the means of all $\bar{\nu}$ measurements for each isotope are listed in Table 6.

9.2 Drifts in Counter Efficiency

Drifts in the counter efficiency were checked continuously during the measurements. Under ideal operating conditions the efficiency remained constant to within 0.05 per cent. for a month or so. Since it was possible to achieve high statistical accuracy in a short period using the Cf252 counter, drifts caused by electronic faults were quickly observed. The few $\bar{\nu}$ results for which there was any uncertainty whatsoever in the efficiency over the measurement period were rejected. Consequently no contribution to the error was considered necessary to account for the effects of drifts in efficiency. The statistical consistency of the individual measurements of $\bar{\nu}$ for a particular isotope supports this view.

TABLE 6

ACCURACY OF $\bar{\nu}$ RESULTS

Effect	U233		U235		Pu239		Pu241	
	Percentage Correction to Exptl. Result	Percentage Error From Effect Listed	Percentage Correction to Exptl. Result	Percentage Error From Effect Listed	Percentage Correction to Exptl. Result	Percentage Error From Effect Listed	Percentage Correction to Exptl. Result	Percentage Error From Effect Listed
1. Statistical Accuracy	–	0.168	–	0.103	–	0.155	–	0.108
2. Counter Drifts	Negligible		Negligible		Negligible		Negligible	
3. Fission by Fast Neutrons	0.000	0.0001	0.000	0.0001	0.000	0.0001	0.000	0.0001
4. Impurities	0.000	0.0013	0.000	0.000	(Pu240) 0.004	0.001	(Pu239) 0.014	0.0014
							(Pu240) 0.17	0.04
							(Pu242) 0.040	0.015
5. Inaccuracy of Fission Counter Location	0.000	0.01	0.000	0.01	0.000	0.01	0.000	0.01
6. False Gates *	0.015	0.005	0.010	0.005	0.02	0.01	0.014	0.005
7. Preferential Detection	0.02	0.02	0.05	0.05	0.0	0.01	0.02	0.02
8. Anisotropy	Negligible		Negligible		Negligible		Negligible	
9. Fission Spectra Differences	−0.51	0.26	−0.55	0.28	−0.34	0.18	−0.32	0.17
10. Dead Time Correction *	−0.20	0.04	−0.30	0.06	−0.05	0.01	−0.10	0.02
11. Double Fission Inhibit	0.000	0.0003	0.000	0.0003	0.000	0.0003	0.000	0.0003
12. Delayed Gamma Rays	0.000	0.10	0.000	0.10	0.000	0.10	0.000	0.10
13. Electronic Errors	0.000	0.03	0.000	0.02	0.000	0.03	0.000	0.02
14. Varying Background	Negligible		Negligible		Negligible		Negligible	
TOTAL	−0.675	±0.33	−0.790	±0.325	−0.366	±0.258	−0.154	±0.232

* Average from several results.

9.3 Fission by Fast Neutrons

The contamination of the thermal neutron beam by fast neutrons was discussed in Section 5. The estimated error caused by the fast neutron component of the thermal neutron beam is of the order of 0.0001 per cent.

Fast neutrons produced by a previous fission event could cause a second fission, but the probability of this occurring is extremely small. Furthermore such an event is eliminated by the double fission inhibit feature of the electronics.

9.4 Impurities

The isotopic analyses of the fissile materials are given in Table 3. The only significant contaminants in U233 and U235 were U234 and U238 but neither U234 nor U238 undergo thermal neutron fission. The small quantity of U235 (0.05 per cent.) in the U233 sample was not sufficient to warrant any correction.

The Pu239 sample contained 0.17 per cent. by weight Pu240 which undergoes spontaneous fission. A small correction of 0.004 per cent. was applied to the Pu239 result, assuming a half life of 1.2×10^{11} years and a $\bar{\nu}$ value of 2.15 for the spontaneous fission of Pu240.

Corrections to the Pu241 result were necessary to account for the spontaneous fission of Pu240, Pu242, and Am241 and for the neutron induced fission of Pu239. The Pu240 and Pu242 contamination introduced corrections of $+0.17 \pm 0.04$ per cent. and $+0.040 \pm 0.015$ per cent. respectively. The contribution of spontaneous fission of Am241 to the Pu241 result was minimized by isotopic separation of the sample before use. Thus the only correction arose from the formation of Am241, by decay of Pu241 following the separation. Two measurements exist for the spontaneous fission half life of Am241; 3.8×10^{10} years (Armani and Gold 1965) and 2.3×10^{14} years (Druin and Flerov 1964). Assuming the first figure, corrections of +0.01 to +0.05 per cent. were estimated for the increased amount of Am241 in the Pu241 foil. However, recent work at the A.A.E.C. is consistent with a half life of 2.3×10^{14} years for spontaneous fission of Am241. On this basis the correction becomes so small that it has been ignored.

A correction of +0.01 per cent. was applied to the Pu241 result to remove the effect of the Pu239 contamination. It has been estimated assuming the $\bar{\nu}$ values measured in the present experiment.

9.5 Inaccuracy of Fission Counter Location

The error introduced by the inaccuracy of the fission counter location was discussed in Section 7 and estimated to be of the order of 0.01 per cent.

9.6 False Gates

False gates were initiated by a coincidence between noise or alpha pile-up pulses in the fission counter and background radiation in the scintillator tank. Corrections produced by false gates were estimated from the background count rate and the false fission counter pulses using the coincidence resolving time of 21 ns.. The corrections in all cases were very small ($\leqslant$ 0.05 per cent.).

9.7 Fission Fragment Detection Efficiency

Fission fragment detection efficiency was reduced by three effects:

(a) Loss of fission fragments in the fissile foil (negligible for Cf252, 3.5 per cent. for U235).

(b) Loss of fission fragments through pulse levels being below the detector bias ($\leqslant$ 1 per cent. in all cases).

(c) Loss of fission events produced by the lack of a coincident scintillator pulse ($\approx$ 0.9 per cent. in all cases).

Diven and Hopkins (Private communication) have attempted to measure the effect of (a) on $\bar{\nu}$ measurements by interspersing Cf252 in a U238 foil and comparing the $\bar{\nu}$ value obtained with this foil with that obtained using a weightless foil. For a U238 foil thickness of 1.2 milligrams cm^{-2} they found identical results within a statistical accuracy of 0.3 per cent.

Recently, Condé and Holmberg (1965) investigated the effect more exhaustively and found the variation in $\bar{\nu}$ for Cf252 covered by various thicknesses of U238. Corrections were applied to the present $\bar{\nu}$ results on the basis of their Cf252 corrections assuming the effect is the same for U233 etc. as for Cf252. The corrections are listed in Table 6. Errors equal to the corrections applied were assumed.

An attempt was made to calculate the effect produced by fragment loss in the case of U235, using the data of Milton and Fraser (1964, 1965) and that of Rossi and Staub (1949). Although the calculation was crude, it indicated that the correction was of the order of that obtained from the curve of Condé and Holmberg.

Although a direct measurement for (b) was not possible, it was estimated from the shape of the bias curve that $\leq$ 1 per cent. of the fission fragments escaping from the fissile foil into the counting gas created pulses which were lost below the detector bias. It is possible that the $\approx$ 1 per cent. lost might have a different effective $\bar{\nu}$ to that of the 99 per cent. detected, since $\bar{\nu}$ is correlated with fission fragment kinetic energy.

For the type of fission counter used, virtually no correlation exists between output pulse height and fission fragment energy because of the close plate spacing and the use of methane as the counting gas. Variation in output pulse height was caused almost entirely by different track lengths in the counting gas.

The lack of a correlation was demonstrated experimentally by measuring the apparent $\bar{\nu}$ for the spontaneous fission of Cf252 as a function of the proportion of fission events detected. As reported in Section 7, no variation was observed between fission fragment detection efficiencies of 98 and 60 per cent, and that for less efficient fragment detection the variation in apparent $\bar{\nu}$ for Cf252 was still minute. As a further precaution all fission counters were operated at the same bias level during the measurements and therefore presumably with the same percentage fragment loss. Thus any unmeasureable effect on the Cf252 calibrations was produced either in part or total in the other isotope calibrations. On the basis of the above arguments, no contribution to the experimental error seems necessary to account for the 1 per cent. or so fragment loss below the fission counter discrimination level.

A small proportion (0.9 per cent.) of the fission fragments was lost because of the lack of a coincident scintillator pulse. Two effects contribute to this loss:

(a) The high resolution of the triple coincidence arrangement on the scintillator photomultiplier tube outputs caused the rejection of approximately 0.6 per cent. of the prompt gamma ray signals. There is no correlation between this effect and $\bar{\nu}$.

(b) The lack of a prompt scintillator signal (0.3 per cent.), which could influence the $\bar{\nu}$ results if there is a strong correlation between fission gamma ray energy and mass ratio. The evidence of Maier-Leibnitz et al. (1965) suggests that such a correlation is not observed except for symmetric fission which is most improbable in any case. An error from this source would be very small and was ignored.

9.8 Anisotropy of Fission Fragment Detection

The directions of fission fragment recoil and neutron emission are related since neutrons tend to be emitted in the same direction as the moving fragments. The scintillation counter efficiency is not independent of neutron direction because of the axial tube, and hence $\bar{\nu}$ for fragments travelling along the axis will be less than $\bar{\nu}$ measured for other directions. For both spontaneous fission and thermal neutron induced fission the fragments are emitted isotropically and therefore the axial tube has no effect on the measurements of $\bar{\nu}$. Nevertheless, the fission counter used in this experiment

tends to detect preferentially those fragments which have a long track length within the counting gas and which therefore tend to be perpendicular to the direction of the neutron beam. Those fragments causing pulses which are not detected above the discrimination bias are most probably emitted in the direction of the neutron beam and therefore along the scintillator tank axial tube. An error could then be introduced in these relative measurements if the angular correlation of neutron emission with fragment direction in the laboratory system varied between Cf252 and the isotopes measured, namely U233, U235, Pu239, and Pu241. This effect appears to be quite small and has been ignored.

9.9 Fission Spectra Differences

Corrections were necessary to the $\bar{\nu}$ values to account for differences between the fission neutron spectrum of each measured isotope and that of the standard, since the response of the detector was energy dependent. Numerous experiments have shown that fission neutron spectra may be accurately described by a Maxwellian distribution $\sqrt{E}\exp(-E/T)$ in which T is a parameter describing the average neutron energy in the laboratory system, $\bar{E} = 3T/2$

The variation in the mean detection efficiency of the scintillator for fission spectra, characterized by various $\bar{E}$ values, was calculated using the efficiency response figures in Table 4. (See Section 7.3). Corrections to each of the four measured $\bar{\nu}$ values were made using the calculated variation with $\bar{E}$ and estimates of $\bar{E}$ for each isotope based on Terrell's (1962) semi-empirical relationship $\bar{E} = 0.74 + 0.653\,(\bar{\nu}+1)^{1/2}$ and the present measured $\bar{\nu}$ values. The corrections are listed in Table 6 (see Section 9). Large errors of 50 per cent. on these corrections have been assumed since there is considerable disagreement between the experimental $\bar{E}$ values and because the energy response figures for the scintillator tank were not confirmed experimentally.

9.10 Dead Time Correction

Table 6 (see Section 9) lists the overlap corrections that have been made in each of the cases U233, U235, Pu239, and Pu241. The values are averages since measurements were made at a variety of reactor powers and therefore with a variety of background count rates. The different reactor powers used account for the fact that the corrections are not necessarily related to the $\bar{\nu}$ result. For example, the average correction necessary for the Pu241 results (0.90 per cent.) is smaller than that for the Pu239 results (0.95 per cent.) since a higher reactor power was used in the latter cases. To determine the error introduced by using an incorrect dead time, it is necessary to consider the relative corrections for Cf252 and the particular isotope. For example, the relative correction in the case of U235 is 0.25 per cent. and it is the error in this that is significant.

A number of overlap corrections were made using the maximum conceivable limits of 0.0080 and 0.0053 for k_{nn} and 0.00425 and 0.00300 for k_{nB} and k_{BB}, the dead time correction parameters. The results of these calculations indicated that the relative overlap corrections were accurate to approximately 20 per cent. The relative error has therefore been estimated to be about 0.05 per cent. of $\bar{\nu}$ in the case of U235 and 0.01 per cent. in the case of Pu239.

The calculation of the overlap correction itself is accurate to 0.003 per cent. of $\bar{\nu}$ ignoring limitations introduced by statistical limitations of the various F'_ℓ and B'_x figures.

9.11 Additional Fissions Occurring During the Gate

In the case of Cf252 there was a 0.60 per cent. probability that a second fission event would occur during the counting cycle. On these occasions all information in the temporary store was discarded and both events ignored.

Nevertheless the double fission inhibit feature did not operate immediately and there was a finite time after the first fission event when it was inoperative. This time was designed to be very small, namely 50 ns. More significant than this is the resolving time of the liquid scintillator tank of 73 ns. During the 73 ns after a first fission event a second fission event cannot be detected by the liquid scintillator tank. The error introduced by the inability of the electronics to detect a second fission event in this 73 ns period was estimated to be 0.0003 per cent.

9.12 Delayed Gamma Rays

An error would be introduced into the relative $\bar{\nu}$ measurements if there is a significant delayed gamma ray component accompanying fission, detectable above the scintillator discriminator level, and if the magnitude of this component is not directly proportional to $\bar{\nu}$. Sund and Walton (1966) investigated the delayed gamma ray components accompanying the neutron and photo fission of U235 and Pu239. They attributed the delayed fission gamma rays in the 0–500 μs period after fission to the decay of four isomeric states produced by the fission process. The properties of these four states are tabulated below.

TABLE 7

ISOMERIC STATES PRODUCED IN THE NEUTRON AND PHOTO-FISSION OF U235 AND Pu239

Isomer Half Life (μs)	Energies of Cascade Gamma Rays (keV)
80	1260, 450
54	850, 250
32	990, 710
4	> 510

Preliminary measurements of the delayed gamma ray component accompanying the spontaneous fission of Cf252 were made for the 0–30 μs period following fission by Allen and Boldeman (A.A.E.C. Unpublished). The measured intensity versus time relationship for Cf252 is consistent with the existence of the four states in Table 7.

The magnitudes of the delayed gamma ray contributions to the present measurements of $\bar{\nu}$ for U233, U235, Pu239, and Pu241 have been estimated from the data above and from measured curves of scintillator efficiency versus gamma ray energy for two photomultiplier tube E.H.T. settings equivalent to 83 and 85 per cent. neutron detection efficiencies (Table 8). The efficiency values 83 and 85 per cent. were those before dead time correction etc. It is assumed here that the contributions are the same for U233 and U235 and also for Pu239 and Pu241. The gamma ray energy of the 4 μs isomeric state is unknown. Two estimates of this contribution were made assuming energies of 700 keV and 1500 keV for E_γ. The total contributions listed in Table 8 vary between the two stated values, depending upon the variation of E_γ between 700 and 1500 keV.

It can be seen from Table 8 that the delayed gamma ray contributions are significantly smaller for an 83 per cent. neutron detection efficiency setting than for the 85 per cent. setting and it was for this reason that all $\bar{\nu}$ measurements were made at the lower efficiency of 83 per cent.

The important feature of the delayed gamma contributions, apart from their small magnitude, is that in all cases they are proportional to $\bar{\nu}$ and so no correction is necessary to the relative $\bar{\nu}$ measurements. Nevertheless, an error of 0.1 per cent. was attached to the reliability of the proportionality hypothesis and is included in Table 6.

9.13 Electronic Errors

The coincidence requirements on the photomultiplier tube outputs caused approximately 0.6 per cent. of fission neutron pulses to be rejected, a quantity which was the same for all isotopes. No error was needed to account for this effect. Measurements of relative $\bar{\nu}$ for U235 with a different coincidence resolving time of 110 ns (and hence an increased dead time) confirmed this conclusion.

TABLE 8

SUMMARY OF DELAYED GAMMA RAY CONTRIBUTIONS

TO THE $\bar{\nu}$ MEASUREMENTS

83% Neutron Detection Efficiency					85% Neutron Detection Efficiency				
Contributions of Various Isomeric States in Percentage of $\bar{\nu}$					Contributions of Various Isomeric States in Percentage of $\bar{\nu}$				
Isotope	32,54,80 μs States	4 μs State E_γ = 700 keV	4 μs State E_γ = 1500 keV	Total	Isotope	32,54,80 μs States	4 μs State E_γ = 700 keV	4 μs State E_γ = 1500 keV	Total
U235 } U233 }	0.12	0.03	0.12	0.15–0.24	U235 } U233 }	0.16	0.05	0.17	0.21–0.33
Pu239 } Pu241 }	0.13	0.03	0.12	0.16–0.25	Pu239 } Pu241 }	0.17	0.05	0.17	0.22–0.34
Cf252				≈0.20	Cf252				≈0.30

A systematic difference between the lengths of the neutron and background counting gates could introduce an error into the $\bar{\nu}$ results particularly in the cases where high backgrounds of as much as 0.7 counts/gate existed. The gate lengths were compared by counting background into both counting channels. The results demonstrated that the counting gate lengths were the same to within ± 0.08 per cent. Errors were assessed assuming a 0.08 per cent. contribution to the uncertainty in the mean background rate for each measurement and average errors are listed for each isotope in Table 6.

9.14 Variations in Background

Variations in background during any particular measurement could introduce an error into the assessment of the dead time correction. Since the reactor was the major source of background, the effect was minimized by maintaining constant reactor power to within 1 per cent. during any measurement. Under these conditions the effect on the dead time correction is very small. Furthermore the dead time correction itself is quite small.

10. DISCUSSION OF RESULTS

The present results are compared with previous measurements in Table 9. The values listed are for prompt neutrons only. In two cases (Colvin and Sowerby 1965, and Kalashnikova et al. 1956) where the published figures included the delayed neutron component, this was subtracted using the data of Keepin (1965). Furthermore, all values listed were normalized to $\bar{\nu}$ (Cf252) = 3.784 so that a direct comparison is possible. The discrepancy which exists for the absolute calibration of Cf252 may be ignored for the purposes of the comparison.

Not all measurements were made relative to Cf252. When U235 was the reference, the weighted mean of U235 results (2.418) relative to Cf252 was used.

The errors quoted in Table 9 are the standard deviations relative to Cf252 and do not include any contribution from the error on the assumed Cf252 $\bar{\nu}$ value.

Several of the values listed in Table 9 were obtained from measurements concerned with the variation of $\bar{\nu}$ with incident neutron energy. The question then arises which is the best measurement of $\bar{\nu}$ for fission induced by thermal neutrons, the measured value for thermal or near-thermal neutrons, or the zero energy intercept of the straight line fit to the $\bar{\nu}$-energy dependence curve. The recent data of Meadows and Whalen (1966) indicate that in the case of U235, $\bar{\nu}$ is not a monotonically increasing function of energy but has at least one maximum below 0.5 MeV. Consequently in the present intercomparison, the value for thermal neutron induced fission was chosen as the best measurement of thermal $\bar{\nu}$.

Excellent agreement exists between all listed values of $\bar{\nu}$ for U235. The weighted mean of all results is 2.418 ± 0.005. The present measurement of $\bar{\nu}$ for Pu241 and that of Colvin and Sowerby (1965) are in good agreement although they both do not agree particularly well with the two earlier results. It is possible that the accuracy attributed to these earlier results may have been a little optimistic. Reasonable agreement also exists between the various U233 results.

A small discrepancy appears to exist in the case of Pu239 between the present measurement and that of Colvin and Sowerby. A careful analysis of the present experiment has failed to reveal the source of the discrepancy.

11. DISTRIBUTION OF NEUTRON EMISSION NUMBERS

From each individual measurement of $\bar{\nu}$, the probabilities of emission of ν neutrons per fission event P_ν were calculated in accordance with formulae given by Diven et al. (1956) for values of ν in the range 0 to 10, as follows:

$$P_\nu = \sum_{x=\nu}^{x=10} \frac{x!}{\nu!(x-\nu)!} \left(1 - \frac{1}{\epsilon}\right)^{x-\nu} \left(\frac{1}{\epsilon}\right)^{\nu} D_x \quad ,$$

where ϵ is the neutron detection efficiency of the scintillator and the D_x are the observed neutron

TABLE 9

COMPARISON OF PROMPT $\bar{\nu}$ MEASUREMENTS FOR U233, U235, Pu239, AND Pu241

Experiment	Previous Standard	Modified Standard	$\bar{\nu}$ U233	$\bar{\nu}$ U235	$\bar{\nu}$ Pu239	$\bar{\nu}$ Pu241	Year of Publication
Boldeman and Dalton		$\bar{\nu}$Cf252=3.784	2.492 ± 0.008	2.416 ± 0.008	2.904 ± 0.008	2.947 ± 0.007	1966
Colvin and Sowerby	$\bar{\nu}$Cf252=3.704 (Abs. Meas.)	$\bar{\nu}$Cf252=3.784	2.479 ± 0.015	2.420 ± 0.011	2.874 ± 0.019	2.932 ± 0.027	1965
Mather et al.	$\bar{\nu}$Cf252=3.782	$\bar{\nu}$Cf252=3.784		2.413 ± 0.012			1964
Mather et al.	$\bar{\nu}$Cf252=3.782	$\bar{\nu}$Cf252=3.784	2.534 ± 0.031		2.932 ± 0.034		1965
Hopkins and Diven	$\bar{\nu}$Cf252=3.771 (Abs. Meas.)	$\bar{\nu}$Cf252=3.784	2.481 ± 0.026	2.433 ± 0.022	2.841 ± 0.028		1963
Condé and Holmberg	$\bar{\nu}$Cf252=3.775	$\bar{\nu}$Cf252=3.784		2.422 ± 0.020			1965
Kalashnikova	$\bar{\nu}$U235 = 1	$\bar{\nu}$U235 = 2.418	2.499 ± 0.025		2.890 ± 0.025	2.996 ± 0.030	1956
deSaussure and Silver	$\bar{\nu}$U235 = 1	$\bar{\nu}$U235 = 2.418	2.475 ± 0.025		2.974 ± 0.025	3.126 ± 0.050	1959

probabilities referred to in Section 7. The neutron emission probability distributions for each of the five isotopes U233, U235, Pu239, Pu241, and Cf252 are given in Table 10. Smooth curves are plotted in Figures 11 to 15.

For each distribution the first and second moments about the origin, $\overline{\nu}$ and $\langle\nu^2\rangle_{av}$, the second moment about $\overline{\nu}$, var, and a shape-dependent parameter, 'R', were calculated as:

$$\overline{\nu} = \sum_{\nu=0}^{\nu=10} \nu P_\nu$$

$$\langle\nu^2\rangle_{av} = \sum_{\nu=0}^{\nu=10} \nu^2 P_\nu$$

$$\text{var} = \sum_{\nu=0}^{\nu=10} P_\nu(\nu - \overline{\nu})^2$$

$$R = \frac{\langle\nu^2\rangle_{av} - \overline{\nu}}{(\overline{\nu})^2} .$$

The relevant parameters are listed in Table 10, together with an assessment of the accuracy based on statistical grounds only. The data are in reasonable agreement with previous measurements.

TABLE 10

NEUTRON EMISSION PARAMETERS

Nuclide	U233	U235	Pu239	Pu241	Cf252
$\overline{\nu}$	2.492 ± 0.008	2.416 ± 0.008	2.904 ± 0.008	2.947 ± 0.007	3.784 ± 0.000
$\langle\nu^2\rangle_{av}$	7.416 ± 0.034	7.073 ± 0.032	9.838 ± 0.040	10.063 ± 0.037	15.925 ± 0.007
var	1.099 ± 0.004	1.112 ± 0.004	1.185 ± 0.005	1.173 ± 0.004	1.268 ± 0.002
R	0.7932 ±0.0013	0.7979 ±0.0013	0.8221 ±0.0016	0.8190 ±0.0010	0.8479 ±0.0005
P_0	0.0259 ±0.0010	0.0313 ±0.0060	0.0094 ±0.0010	0.0097 ±0.0010	0.00197 ±0.00008
P_1	0.1526 ±0.0020	0.1729 ±0.0016	0.0990 ±0.0027	0.0877 ±0.0025	0.02447 ±0.00025
P_2	0.3289 ± 0.0034	0.3336 ±0.0029	0.2696 ±0.0034	0.2636 ±0.0030	0.1229 ±0.0005
P_3	0.3282 ±0.0035	0.3078 ±0.0029	0.3297 ±0.0035	0.3343 ±0.0032	0.2707 ±0.0008
P_4	0.1320 ±0.0017	0.1232 ±0.0016	0.1982 ±0.0030	0.2099 ±0.0035	0.3058 ±0.0010
P_5	0.0252 ±0.0020	0.0275 ±0.0020	0.0924 ±0.0040	0.0811 ±0.0040	0.1884 ±0.0007
P_6	0.0045 ±0.0020	0.0038 ±0.0015	0.0119 ±0.0020	0.0112 ±0.0020	0.0677 ±0.0006
P_7					0.0160 ±0.0003
P_8					0.0021 ±0.0002

Note: The errors quoted for the various P_ν have been estimated from experimental reproducibility only.

12. REFERENCES

Armani, R.J., and Gold, R. (1965). – ANL7110, page 23.

Asplund-Nilsson, I., Condé, H., and Starfelt, N. (1963). – Nucl. Sci. and Eng. 16: 124.

Colvin, D.W., and Sowerby, M.G. (1963). – Private Communication referred to by Condé and Holmberg (1965).

Colvin, D.W., and Sowerby, M.G. (1965). – I.A.E.A. Proc. of Symp. on Physics and Chemistry of Fission, Salzburg, 2: 25.

Condé, H., and Holmberg, M. (1965). – I.A.E.A. Proc. of Symposium on Physics and Chemistry of Fission, Salzburg, 2: 57.

Condé, H., and Holmberg, M. (1965). – Arkiv För Fysik, 29: 33.

Cunninghame, J.G., and Kitt, G.P. (1964). – AERE-R4727.

deSaussure, G., and Silver, E.G. (1959). – Nucl. Sci. and Eng. 5: 49.

De Volpi, A., Porges, K.G., and Rush, C.J. (1964). – CONF-481-46.

Diven, B.C., Martin, H.C., Taschek, R.F., and Terrell, J. (1956). – Phys. Rev. 101: 1012.

Diven, B.C., and Hopkins, J.C., Private Communication referred to by Colvin and Sowerby (1963).

Druin, V.A., and Flerov, G.N. (1964). – Spontaneous Nuclear Fission, Physics of Nuclear Fission. Edited by N.A. Perfilov and U.P. Eismont (Israel Program for Scientific Translations, Jerusalem).

Fieldhouse, P., Culliford, E.R., Mather, D.S., Colvin, D.W., MacDonald, R.I., and Sowerby, M.G. (1966). – Private Communication.

Fraser, J.S., and Milton, J.C.D. (1964). – AECL2013.

Hopkins, J.C., and Diven, B.C. (1963). – Nucl. Phys. 48: 433.

Kalashnikova, V.I., Lebedev, V.I., Mikaelyan, L.A., Spivak, P.E., and Zakharova, V.P. (1956). – AEC-tr-2435, page 123.

Keepin, G.R. (1965). – Physics of Nuclear Kinetics, Addison Wesley.

Maier-Leibnitz, H., Schmitt, H.W., and Armbruster, P. (1965). – I.A.E.A. Proc. of Symposium on Physics and Chemistry of Fission, Salzburg, 2: 143.

Marks, A.P. (1962). – Atomic Energy, 5 (4): 9.

Mather, D.S., Fieldhouse, P., and Moat, A. (1964). – Phys. Rev. 133: 1403.

Mather, D.S., Fieldhouse, P., and Moat, A. (1965). – Nucl. Physics, 66: 1.

Meadows, J., and Whalen, J. (1966). – WASH-1068, page 21.

Milton, J.C.D., and Fraser, J.S. (1965). – I.A.E.A. Proc. of Symposium on Physics and Chemistry of Fission, Salzburg, 2: 39.

Moat, A., Mather, D.S., and McTaggart, M.H. (1961). – J. Nucl. Energy, Parts A/B, 15: 102.

Moat, A., Mather, D.S., and Fieldhouse, P.F. (1962). – I.A.E.A. Proc. of Conf. Physics of Fast and Intermediate Reactors, 1: 139.

Rossi, B.B., and Staub, H.H. (1949). – Ionisation Chambers and Counters, McGraw-Hill.

Rush, C.J. (1964). – Rev. of Sci. Inst. 34: 149.

Sund, R.E., and Walton, R.B. (1966). – Phys. Rev. 146: 824.

Terrell, J. (1962). – Phys. Rev. 127: 880.

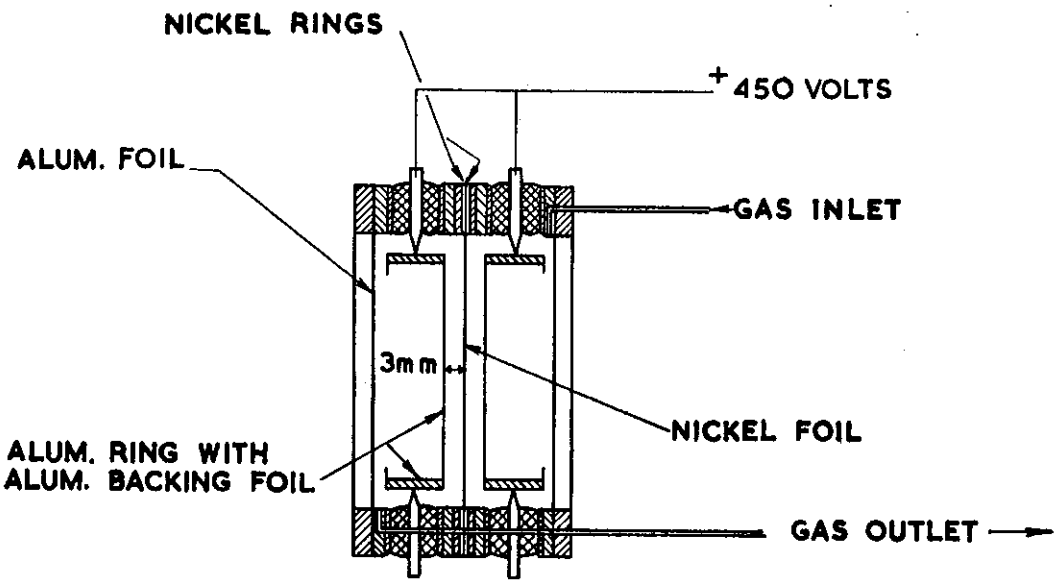

FIGURE 1. FISSION COUNTER

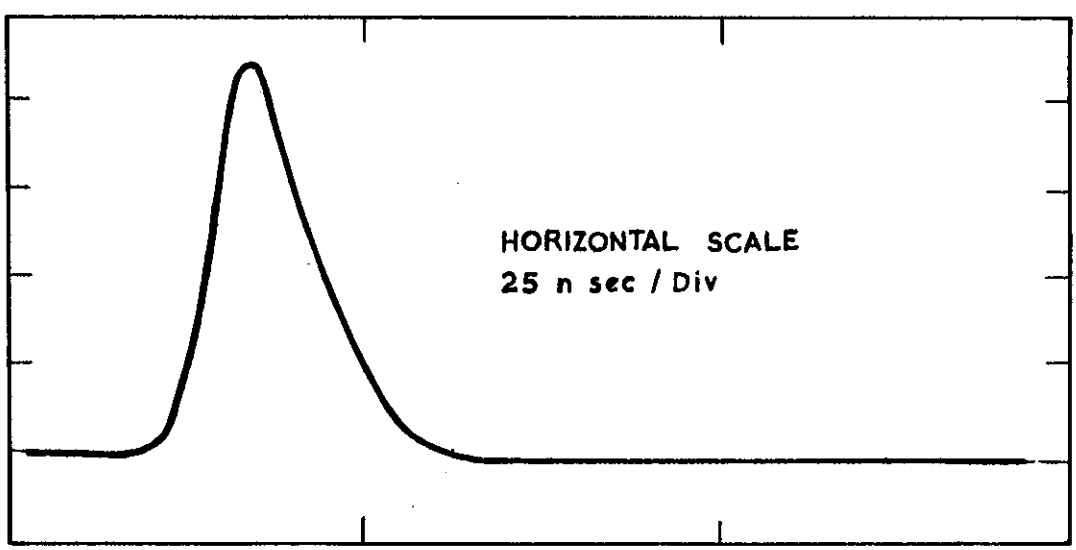

FIGURE 2. FISSION COUNTER PULSE SHAPE

P1077

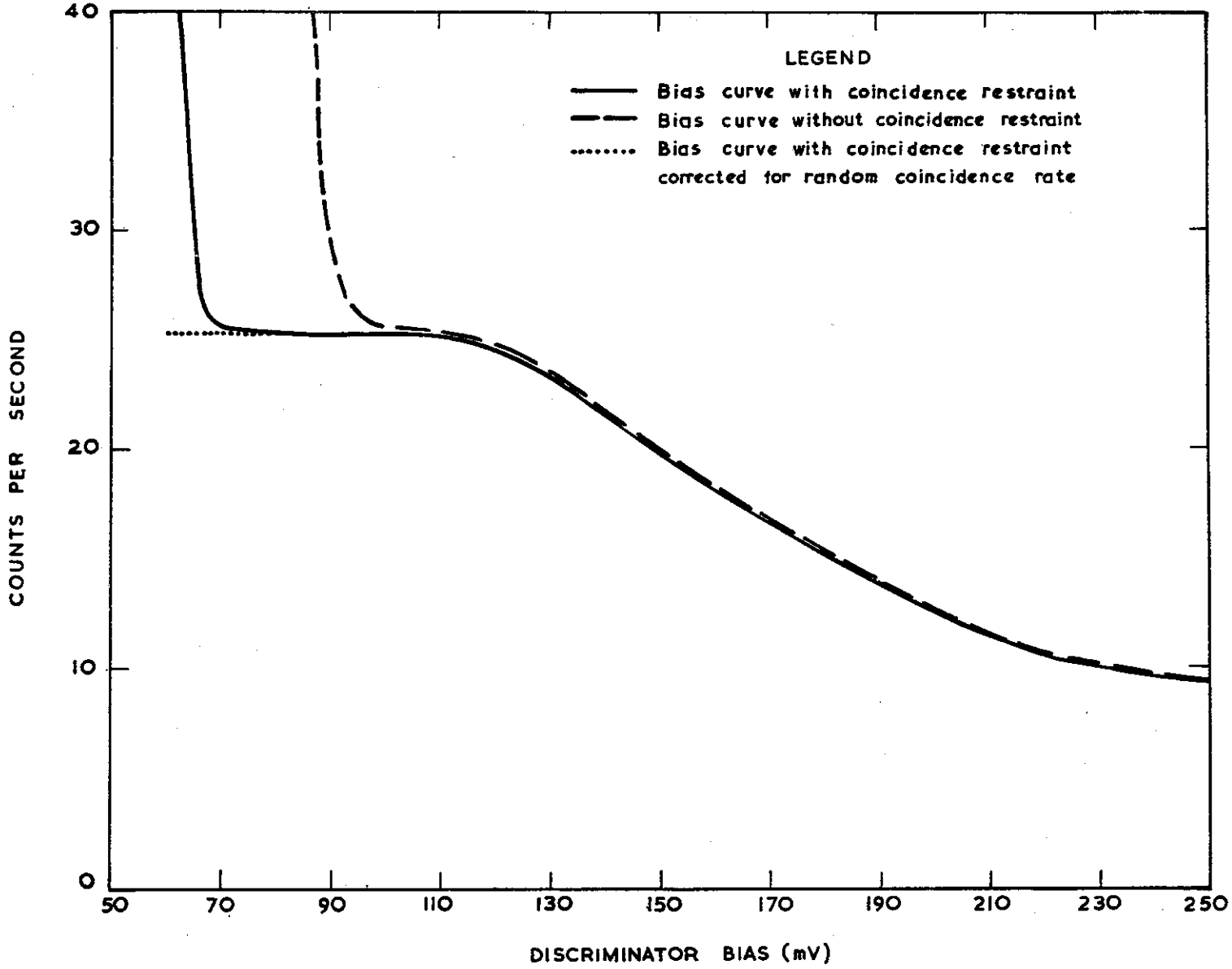

FIGURE 3(a) FISSION COUNTER BIAS CURVE (Cf252), LINEAR SCALE

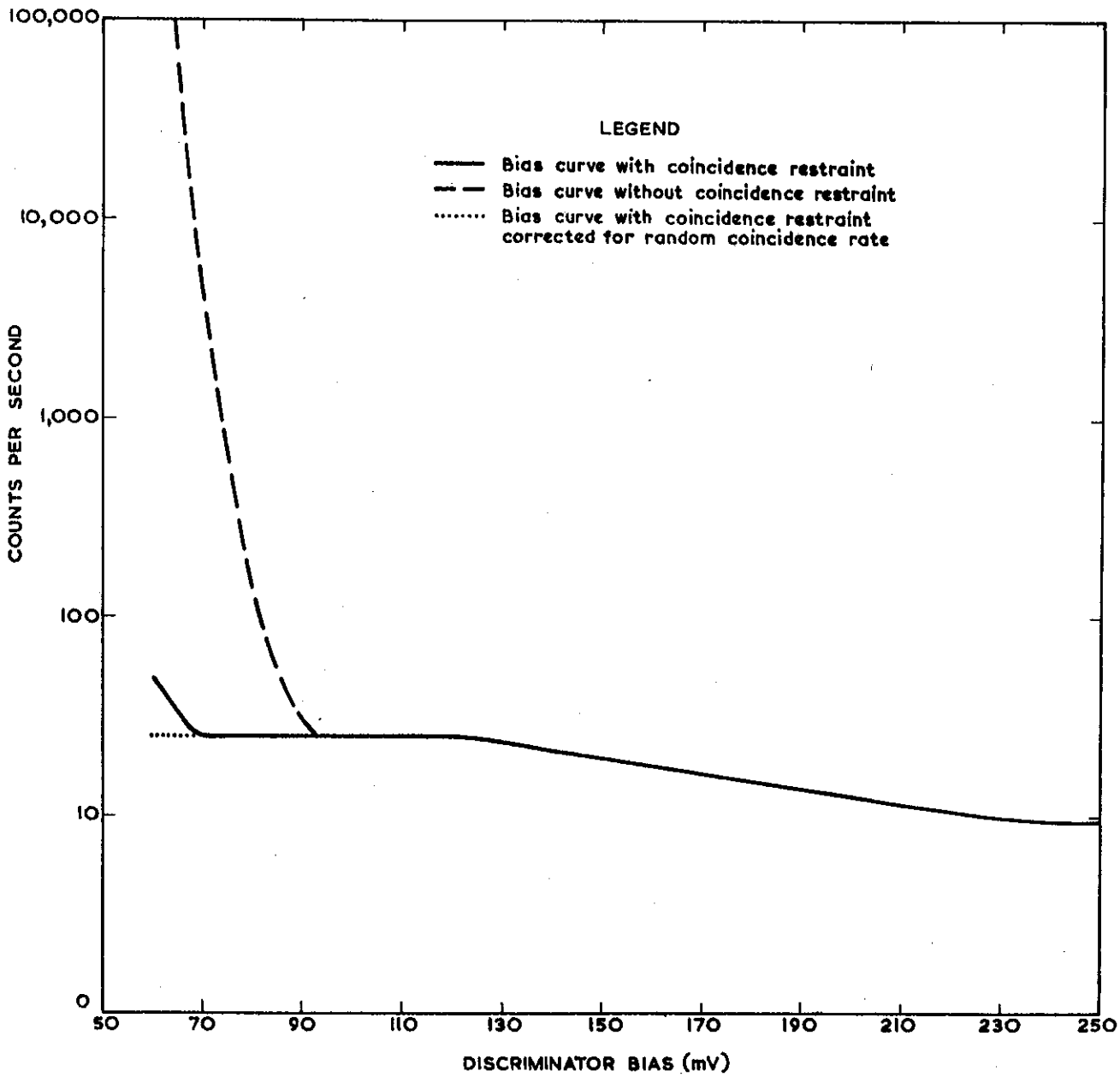

FIGURE 3(b) FISSION COUNTER BIAS CURVE (Cf252), LOGARITHMIC SCALE

P1077

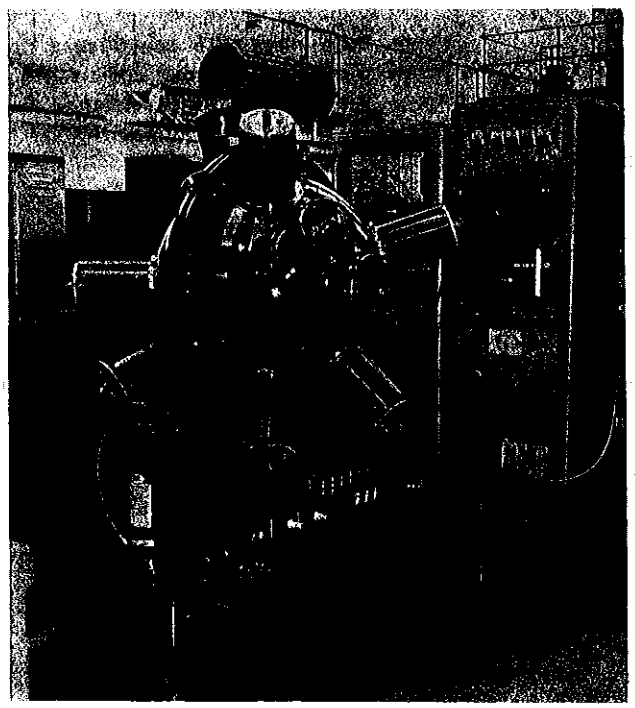

FIGURE 4. THE LIQUID SCINTILLATOR TANK

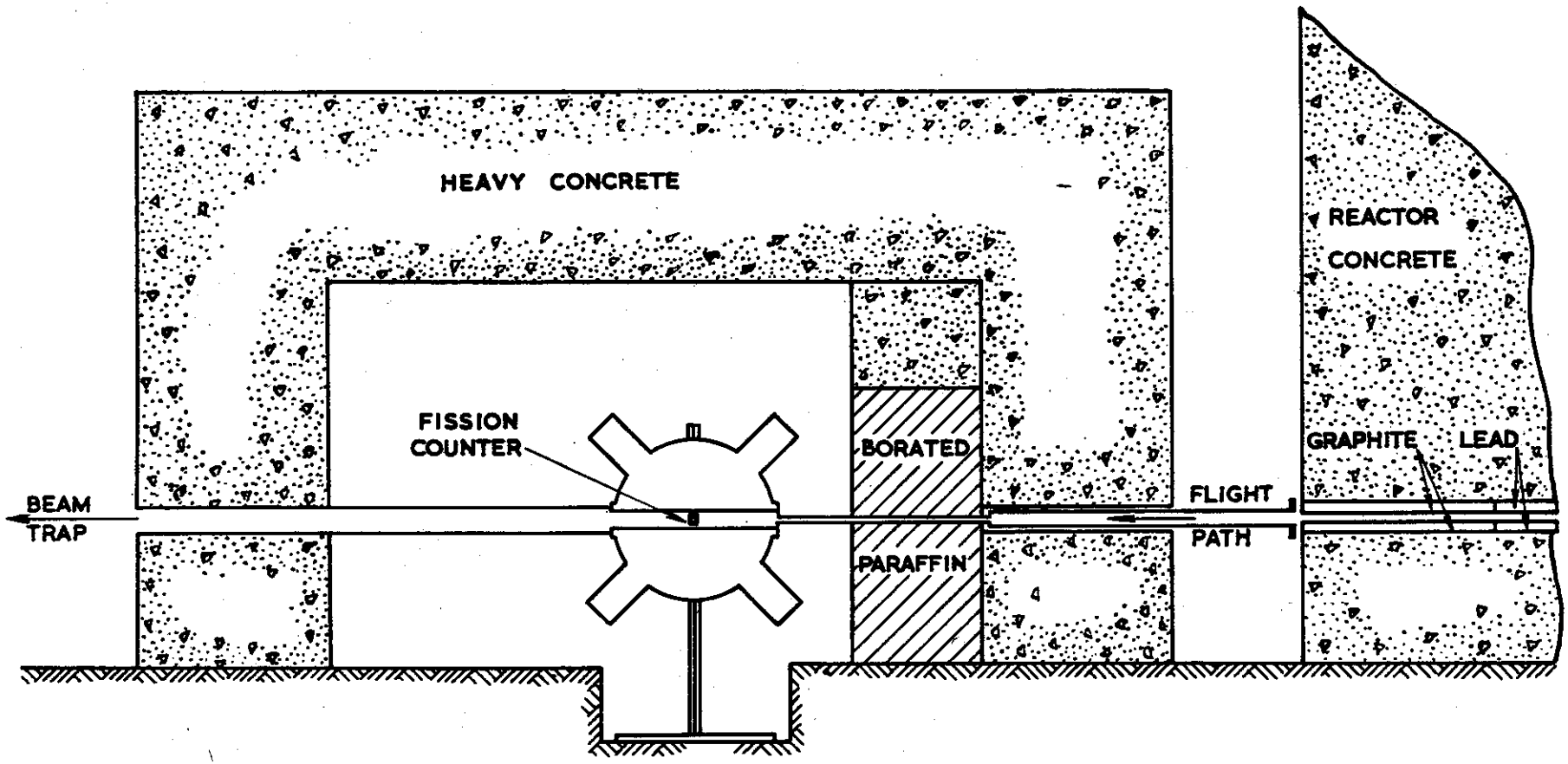

FIGURE 5. NEUTRON COLLIMATOR AND SHIELDING

P1077

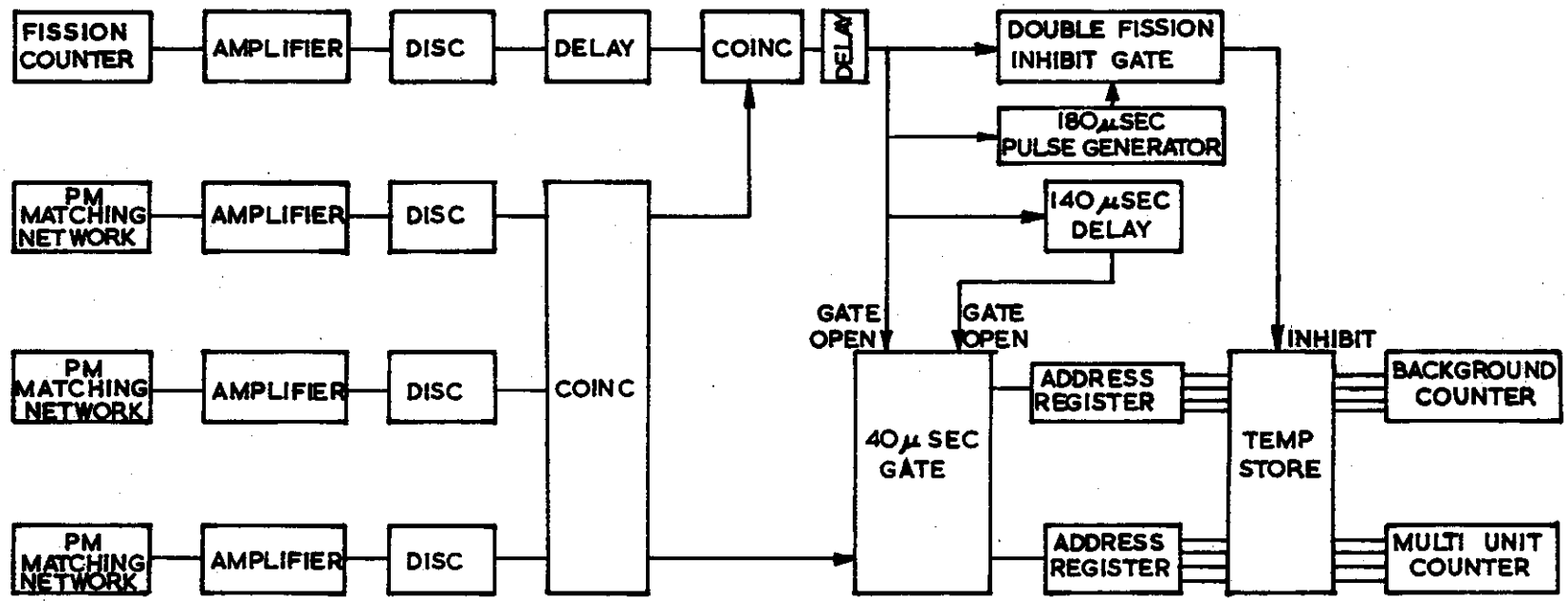

FIGURE 6. BLOCK DIAGRAM OF ELECTRONICS

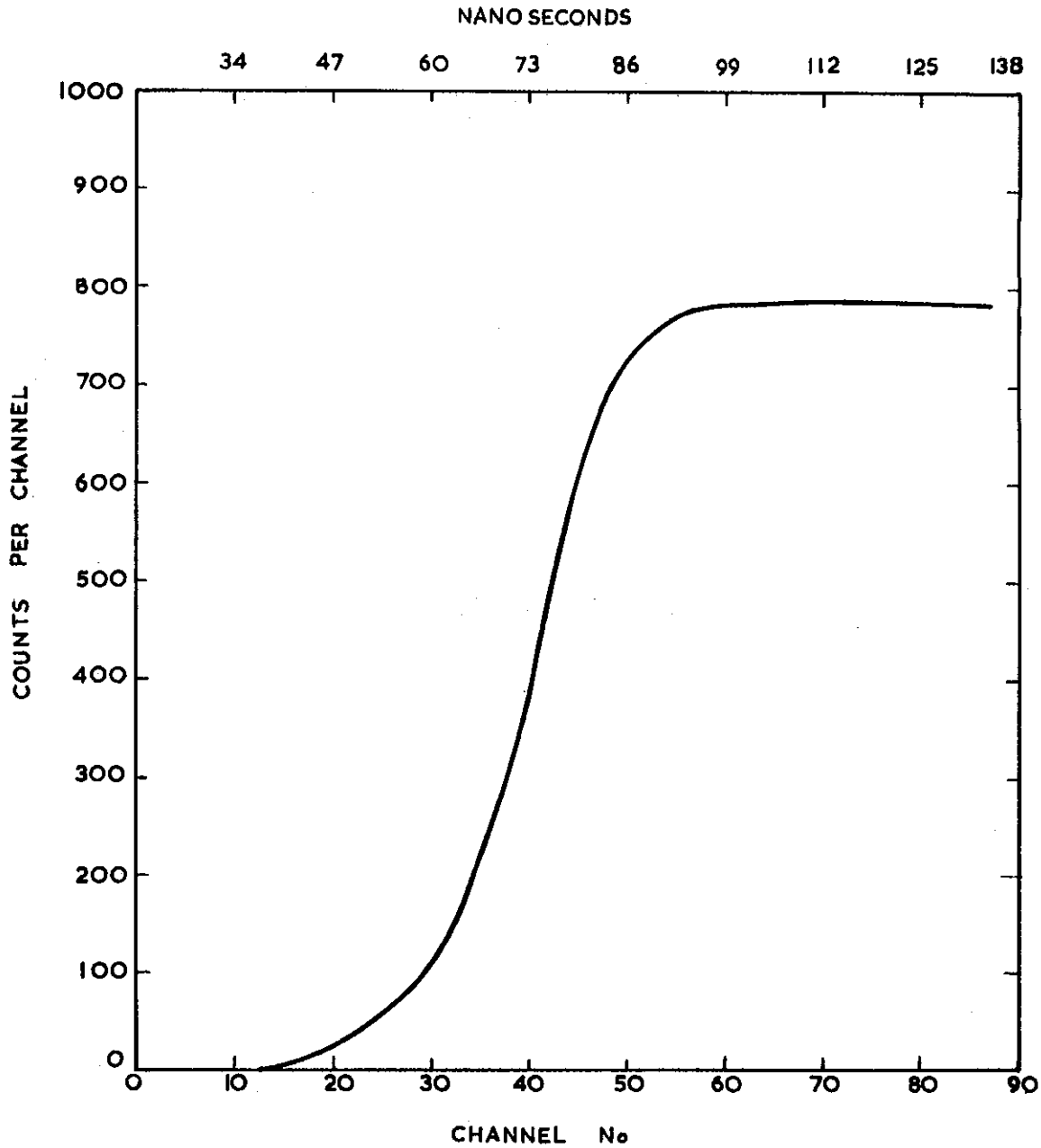

FIGURE 7. TIME DISTRIBUTION BETWEEN TWO PULSES

P1077

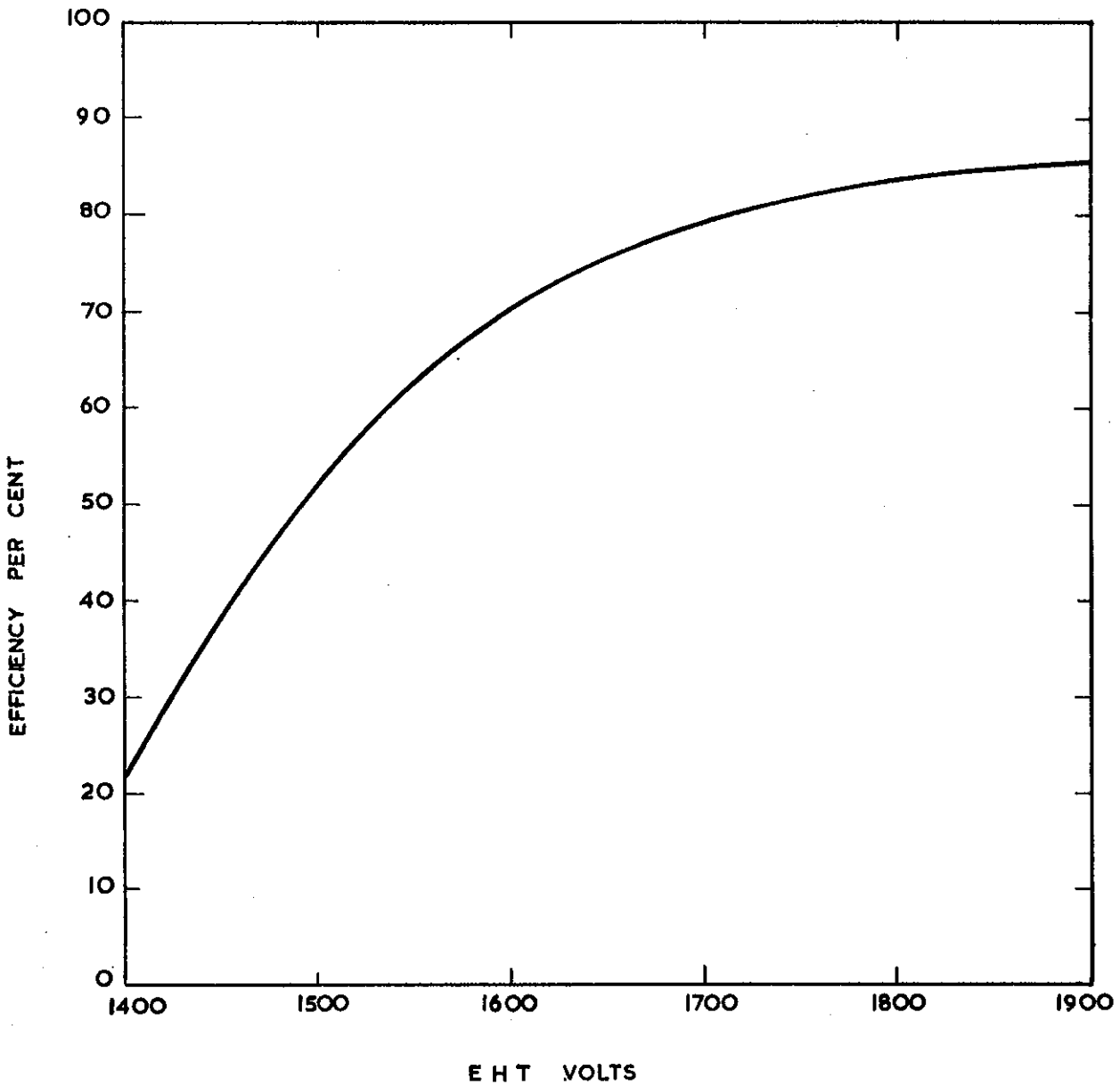

FIGURE 8. NEUTRON DETECTION EFFICIENCY VERSUS E.H.T. TO BALANCING NETWORK

P1077

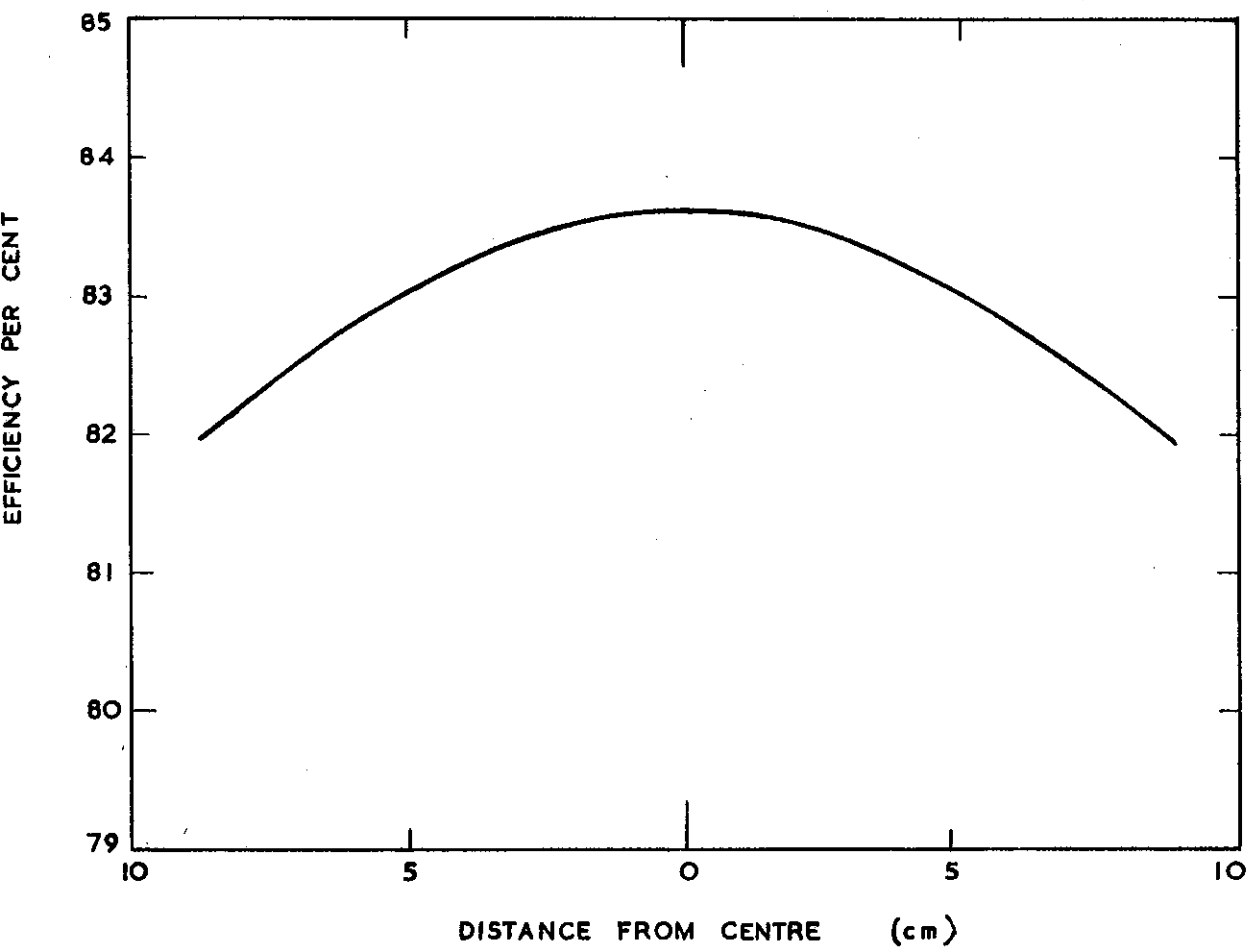

FIGURE 9. DETECTOR EFFICIENCY VERSUS FISSION COUNTER POSITION

P1077

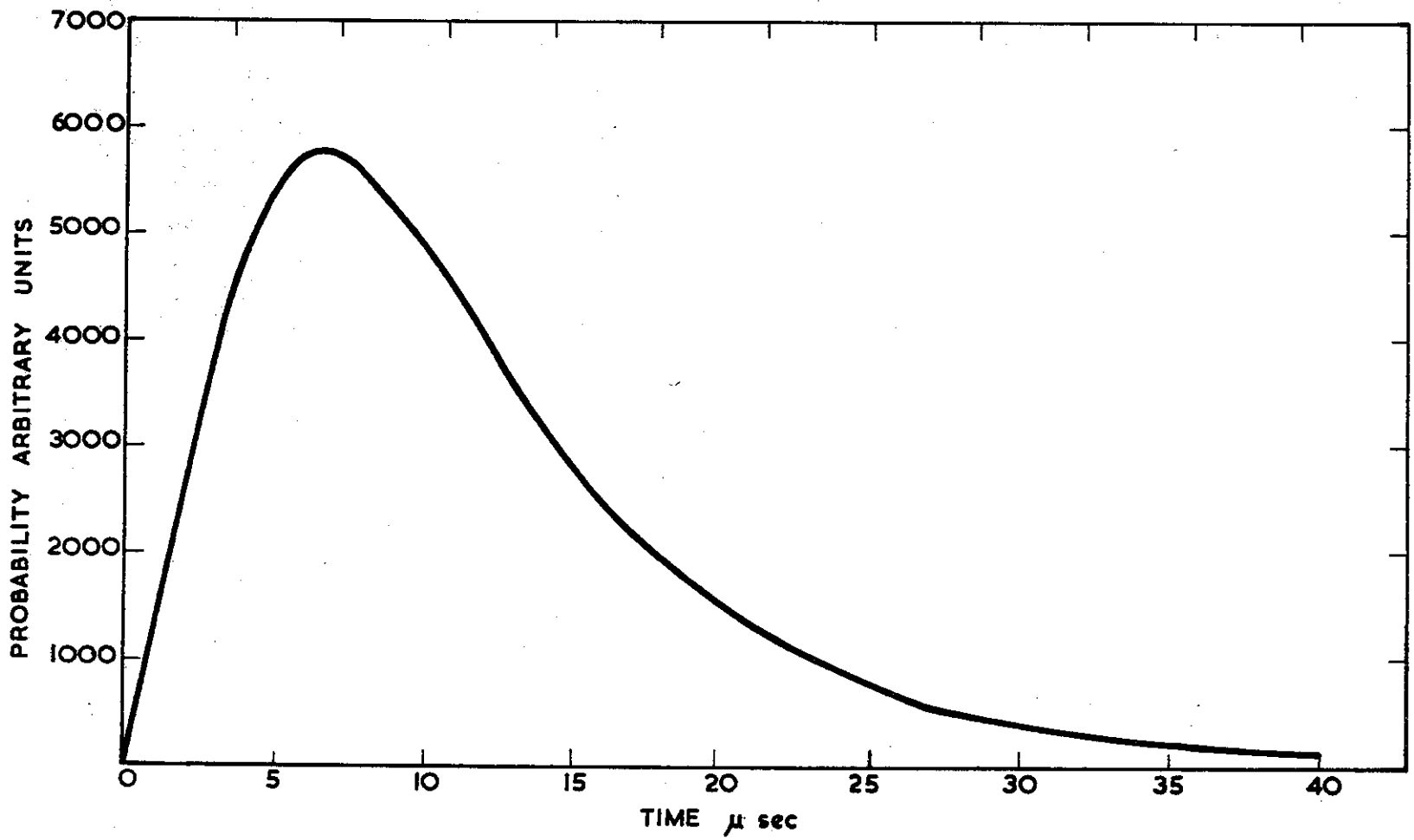

FIGURE 10. TIME DISTRIBUTION OF NEUTRON CAPTURE

P 1077

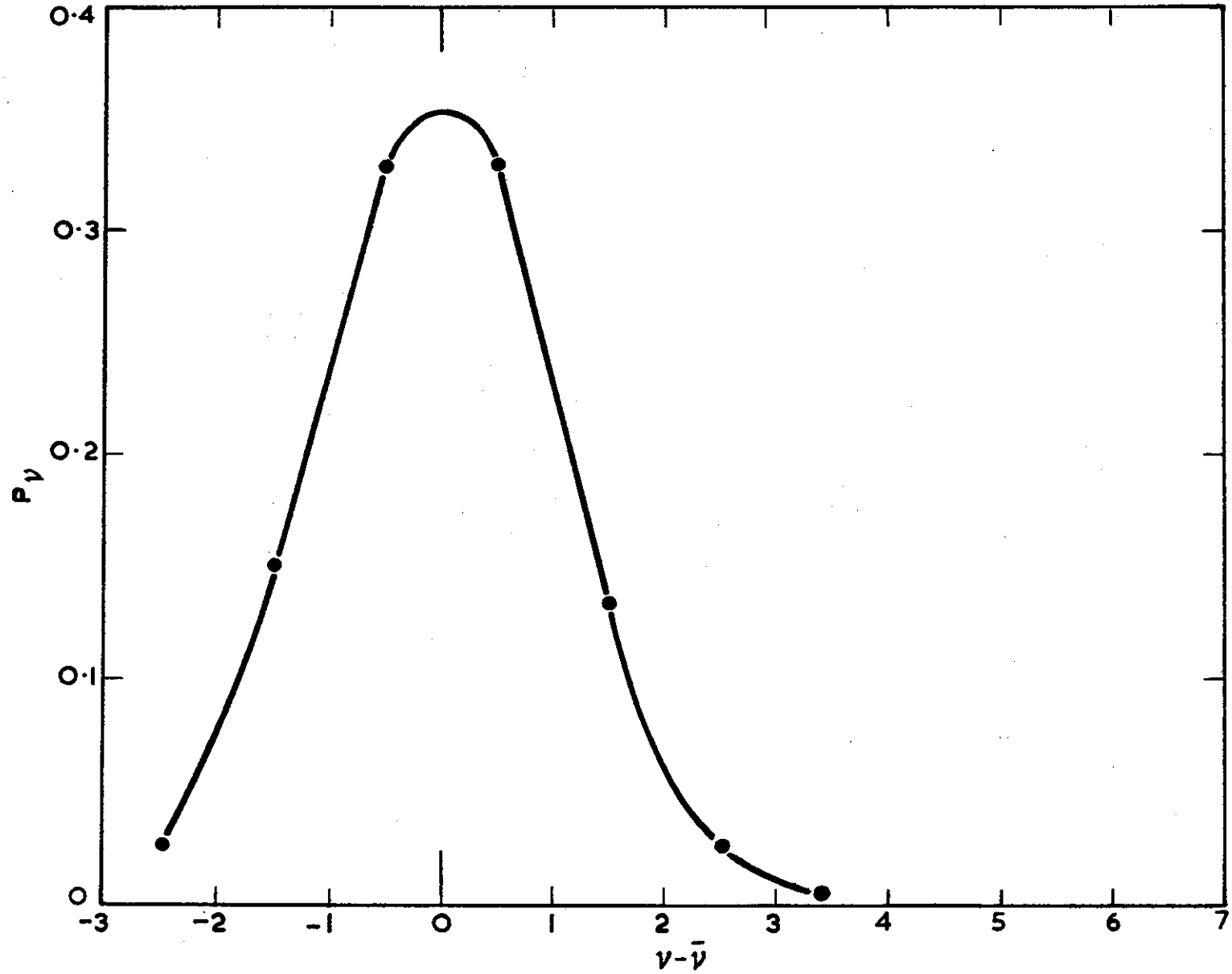

FIGURE 11. NEUTRON EMISSION PROBABILITY DISTRIBUTION FOR U233

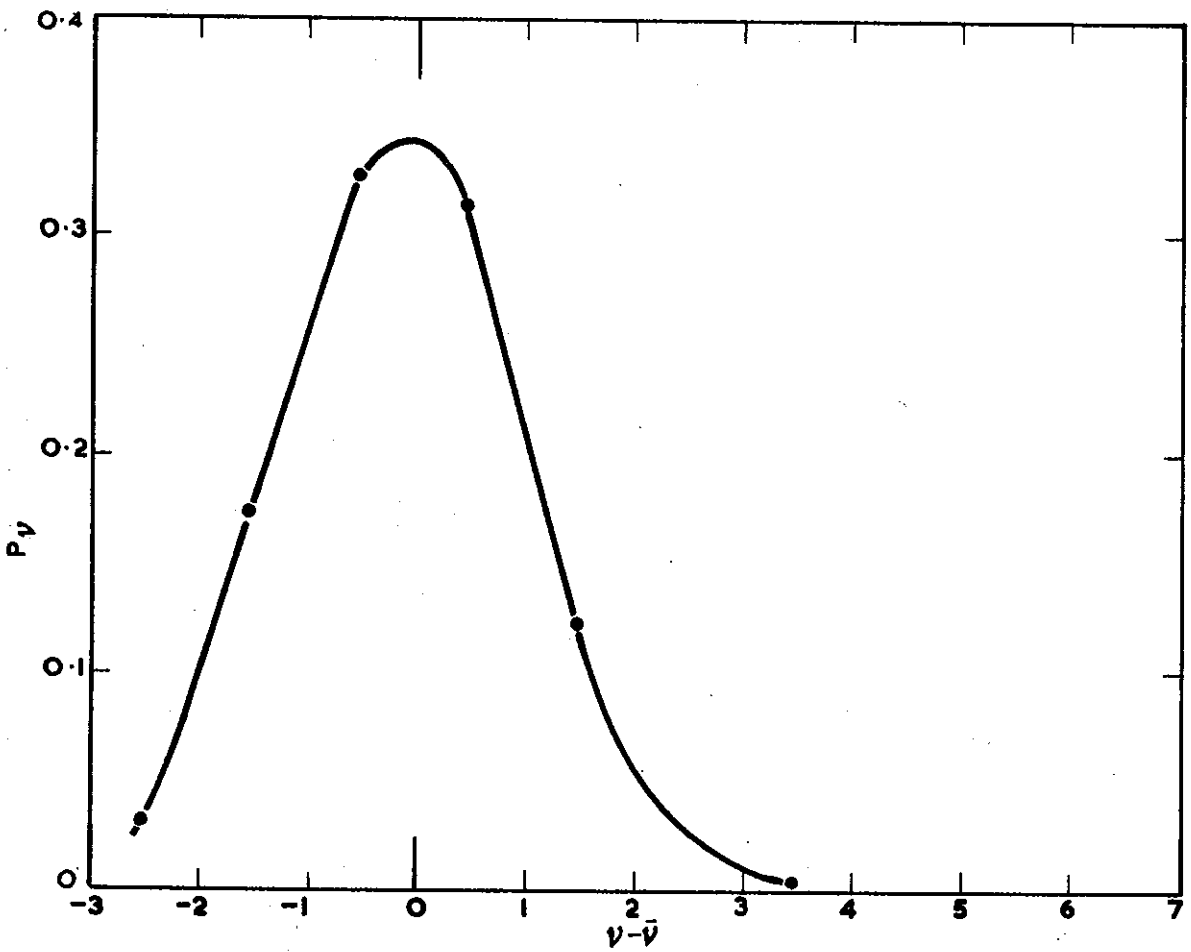

FIGURE 12. NEUTRON EMISSION PROBABILITY DISTRIBUTION FOR U235

P1077

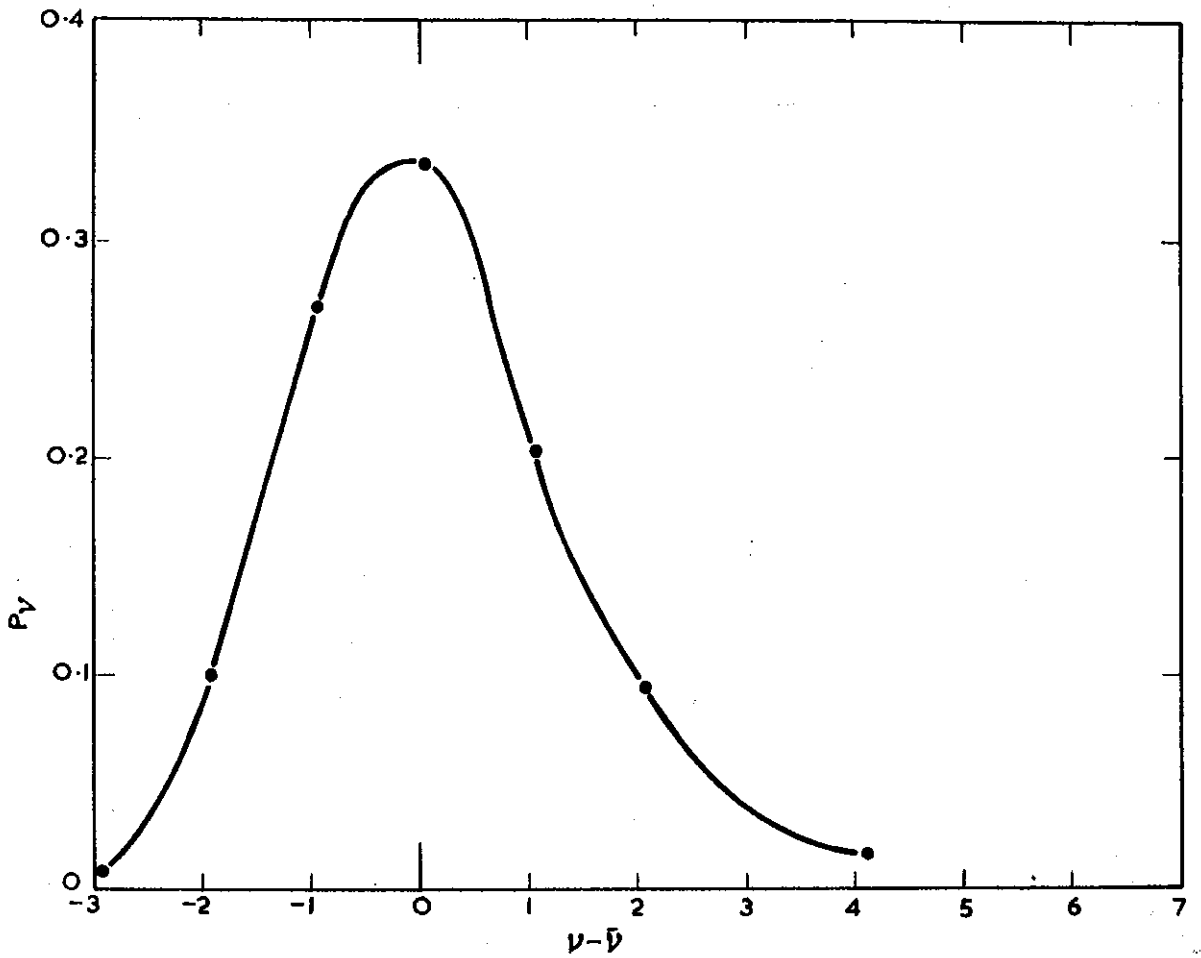

FIGURE 13. NEUTRON EMISSION PROBABILITY DISTRIBUTION FOR Pu239

P 1077

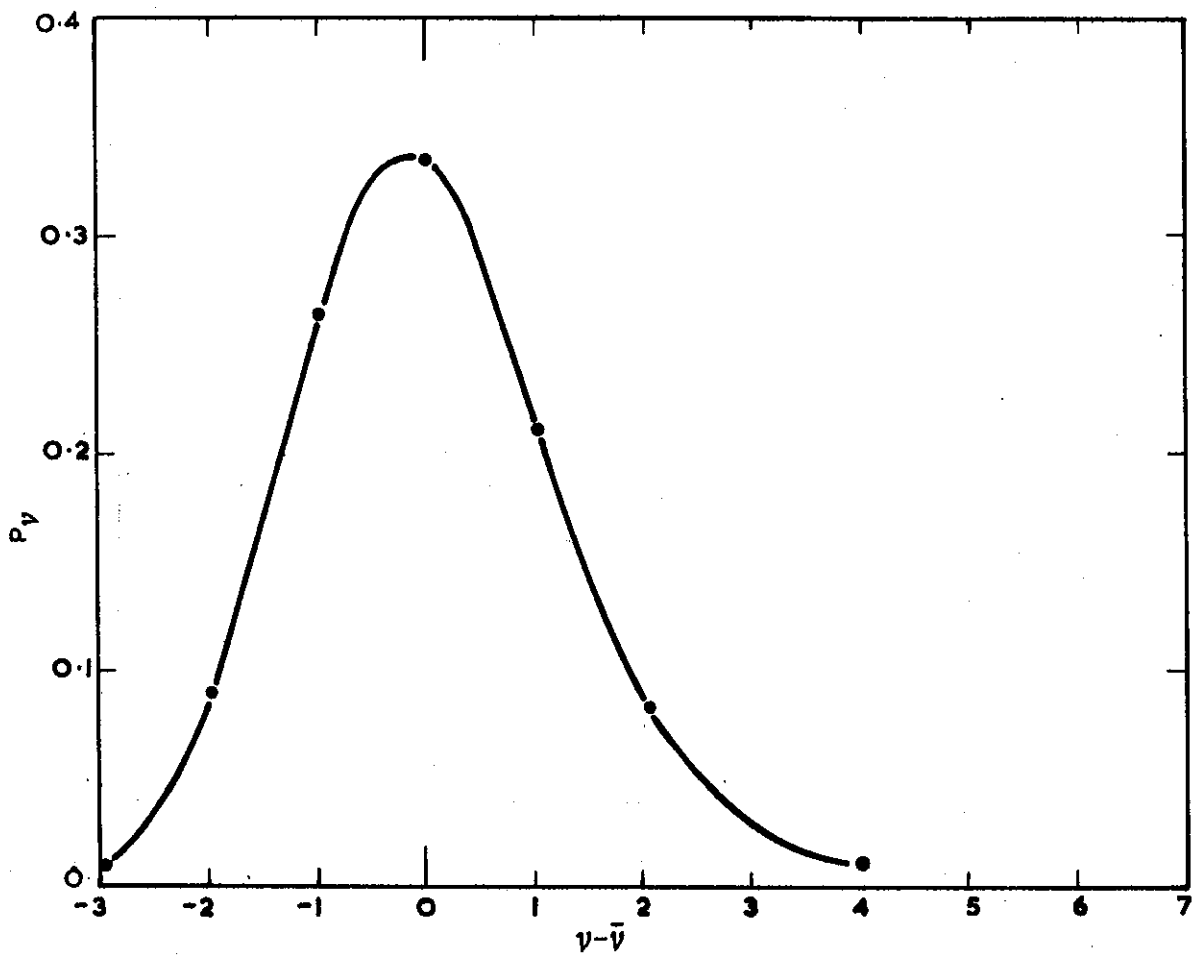

FIGURE 14. NEUTRON EMISSION PROBABILITY DISTRIBUTION FOR Pu241

P1077

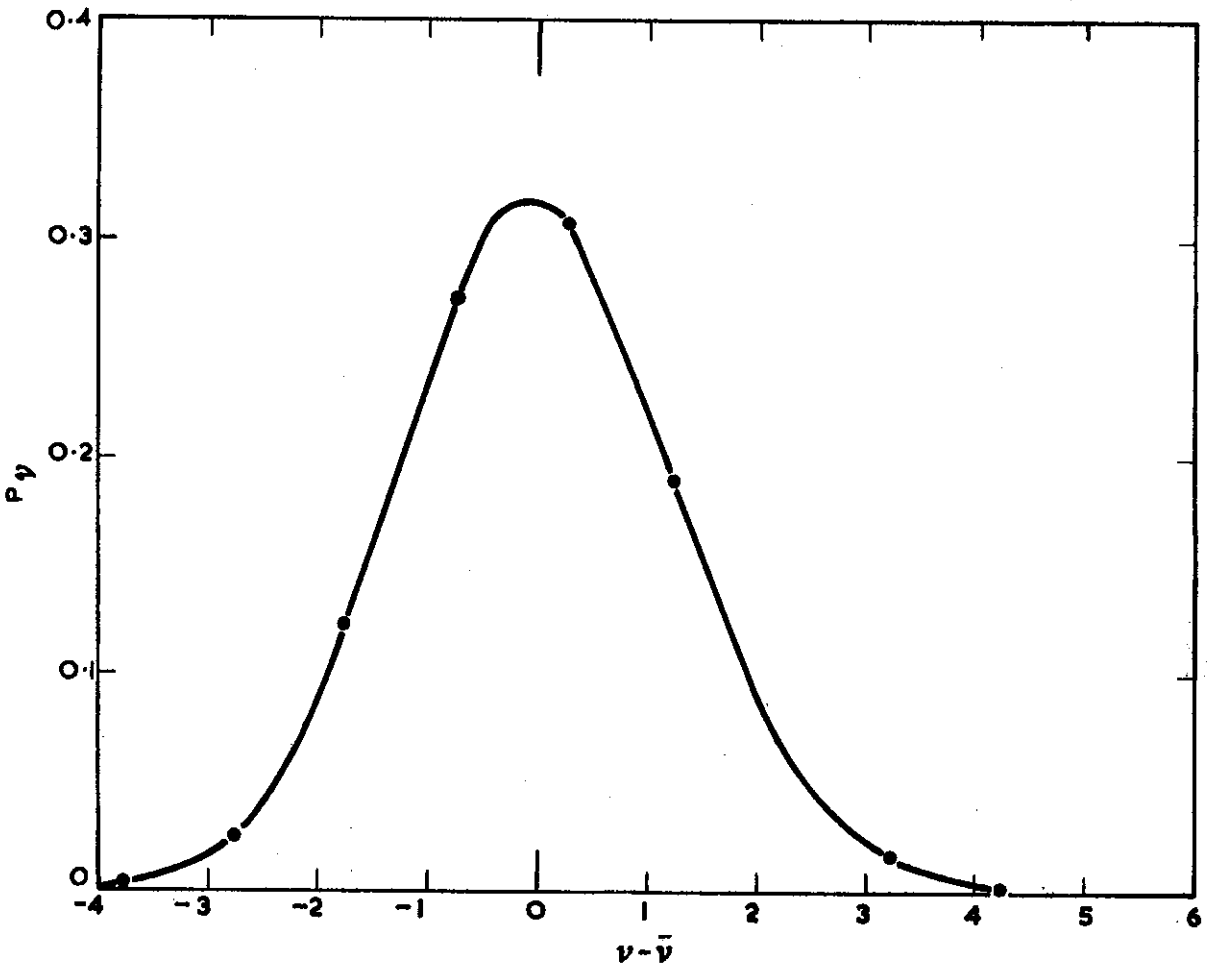

FIGURE 15. NEUTRON EMISSION PROBABILITY DISTRIBUTION FOR Cf252

P1077